GEOPHYSICS, VOL. 69, NO. 4 (JULY-AUGUST 2004); P. 1071–1081, 4 FIGS., 2 TABLES.
10.1190/1.1778249

Matrix propagator method for layered porous media: Analytical expressions and stability criteria

Jeroen Jocker*, David Smeulders*, Guy Drijkoningen*, Caroline van der Lee*, and Alina Kalfsbeek*

ABSTRACT

We fully expand the Thomson-Haskell propagator matrix method to obtain closed-form analytical expressions for the reflectivity and transmittivity of a horizontally stratified poroelastic Biot-type medium that is bounded from above and below by fluid half-spaces. Stable and unstable regions of the propagator matrix method are determined by means of comparison with the inherently stable reflectivity method. It was found that the stability is mainly determined by the imaginary part of the vertical wavenumber of the Biot slow wave.

INTRODUCTION

Reflection and transmission of elastic waves propagating through successive layers of fluid-filled porous solids is inherent to many theoretical and practical applications such as seismology, nondestructive testing, and underwater acoustics.

Description of elastic wave propagation through nonporous layers was introduced by Thomson (1950) and Haskell (1953), who proposed a matrix method that transfers stresses and displacements through successive layers. Although this matrix method can be used in principle, numerical methods based on its direct implementation become unstable in the evanescent regime for high frequencies and large layer thicknesses, and special numerical treatment is required to ensure numerical stability (Kennett, 1983; Lévesque and Piché, 1992). For layered acoustic media with finite thickness, Shapiro et al. (1994) present an extension of the O'Doherty-Anstey formula and effectively characterize a layered acoustic medium by a frequency-dependent velocity anisotropy.

Schmidt and Jensen (1985) proposed a different approach whereby local equations for individual layers are mapped into a global system that comprises all unknowns associated with boundary conditions. In this case, effectiveness depends on the stability of the Gaussian elimination technique used in the numerical computations. A very stable and efficient implementation is the so-called global matrix approach (Schmidt and Tango, 1986). Applications were discussed by, among others, Haartsen and Pride (1997), who treated electroseismic wave propagation, and Gurevich et al. (1999), who used the so-called OASES code to specify some of the layers in the stack as poroelastic materials.

Yet another technique is the reflectivity method (Kennett and Kerry, 1979) that builds up the reflection and transmission matrices iteratively by starting at the top of a lower bounding half-space and adding one layer per iteration until the total stack response is constructed. The recursion is obtained by simple intuitive reasoning and is exact (Pride et al., 2002). In spite of its disadvantages for larger layer thicknesses and high frequencies, the matrix propagator method is still frequently used.

Recently, Wang and Kümpel (2003) presented a fast and powerful numerical scheme to compute poroelastic solutions in a multilayered half-space, based on an extension of the original Thomson-Haskell algorithm. However, the governing poroelastic equations were quasi-static, and inertia terms were neglected.

In this paper, we expand the Thomson-Haskell propagator method to present closed-form analytical expressions for the reflection and transmission coefficients of a multilayered poroelastic medium within the framework of the full Biot theory. The stability of the computations based on a direct implementation of the analytical expressions is tested through comparison with the numerical reflectivity method.

We present the physical model in the next section. Then, the matrix propagator method is discussed briefly, and the analytical expressions for the elements of Haskell's propagator matrix are derived followed by the expressions for reflection and transmission coefficients. We finally discuss the stability of the method and summarize our conclusions.

Manuscript received by the Editor January 23, 2003; revised manuscript received January 9, 2004.
*Delft University of Technology, Center for Technical Geoscience, Department of Applied Earth Sciences, 2628 RX Delft, The Netherlands. E-mail: j.jocker@citg.tudelft.nl; d.m.j.smeulders@citg.tudelft.nl; g.g.drijkoningen@citg.tudelft.nl.

PHYSICAL MODEL

The governing equations for this study are those describing wave propagation in uniformly saturated isotropic porous media (Biot, 1956). It is assumed that for long-wavelength disturbances ($\lambda \gg a$, where λ is the wavelength and a is a characteristic pore scale), we can define average values of the local displacements $\mathbf{u}(\mathbf{r}, t)$ in the solid and $\mathbf{U}(\mathbf{r}, t)$ in the fluid. If we consider a cube of unit size of bulk material (porosity ϕ), we will denote τ_{ij} the forces per unit bulk area applied to that portion of the cube faces occupied by the solid. They are a result of both the fluid pressure p and the intergranular stresses σ_{ij}:

$$\tau_{ij} = -\sigma_{ij} - (1-\phi)p\delta_{ij}, \tag{1}$$

where the Kronecker symbol δ_{ij} reflects the fact that the pore fluid cannot exert nor sustain any shear forces. The total normal tension force per unit bulk area applied to the fluid faces of the cube is denoted τ:

$$\tau = -\phi p. \tag{2}$$

In the case of isotropic materials, the stress-strain relations for, respectively, the solid and the fluid may be written as (Biot, 1956)

$$\tau_{ij} = 2\mu e_{ij} + Ae_{kk}\delta_{ij} + Q\varepsilon_{kk}\delta_{ij}, \tag{3}$$

$$\tau = Qe_{kk} + R\varepsilon_{kk}, \tag{4}$$

where $e_{ij} = 1/2(\partial u_i/\partial x_j + \partial u_j/\partial x_i)$, $\varepsilon_{ij} = 1/2(\partial U_i/\partial x_j + \partial U_j/\partial x_i)$, and where summation over repeated indices is assumed. A, Q, and R are generalized elastic parameters which can be related (under the restriction that the grains in each rock sample are both isotropic and homogeneous) via Gedanken experiments to porosity, bulk modulus of the solid K_s, bulk modulus of the fluid K_f, bulk modulus of the porous drained matrix K_b, and shear modulus μ of both the drained matrix and of the composite (Biot and Willis, 1957):

$$A = \frac{\phi K_b + (1-\phi)K_f\left(1-\phi-\frac{K_b}{K_s}\right)}{\phi_{\text{eff}}} - \frac{2}{3}\mu,$$

$$Q = \frac{\phi K_f\left(1-\phi-\frac{K_b}{K_s}\right)}{\phi_{\text{eff}}},$$

$$R = \frac{\phi^2 K_f}{\phi_{\text{eff}}}, \tag{5}$$

where $\phi_{\text{eff}} = \phi + K_f/K_s(1-\phi-K_b/K_s)$ is some effective porosity. The equations of motion can be written as (Biot, 1956)

$$-\frac{\partial \sigma_{ji}}{\partial x_j} - (1-\phi)\frac{\partial p}{\partial x_i} = \frac{\partial^2}{\partial t^2}(\rho_{11}u_i + \rho_{12}U_i) + b_0 B\frac{\partial}{\partial t}(u_i - U_i), \tag{6}$$

$$-\phi\frac{\partial p}{\partial x_i} = \frac{\partial^2}{\partial t^2}(\rho_{12}u_i + \rho_{22}U_i) - b_0 B\frac{\partial}{\partial t}(u_i - U_i), \tag{7}$$

where the density factors are given by $\rho_{12} = -(\alpha_\infty - 1)\phi\rho_f$, $\rho_{11} = (1-\phi)\rho_s - \rho_{12}$, $\rho_{22} = \phi\rho_f - \rho_{12}$, where we define α_∞ as the tortuosity and ρ_f and ρ_s as the intrinsic fluid and solid densities, respectively. The viscous damping factor is denoted $b_0 = \eta\phi^2/k_0$, with η the fluid viscosity and k_0 the permeability. Assuming harmonic $\exp(i\omega t)$-dependence, the viscous correction factor B was formulated in its generalized form by Johnson et al. (1987) as

$$B = \sqrt{1 + \frac{1}{2}iM\frac{\omega\chi k_0\rho_f}{\eta}}, \tag{8}$$

where M is a dimensionless number that depends only on the pore geometry:

$$M = \frac{8\chi k_0}{\Lambda^2}. \tag{9}$$

Here, χ is the formation factor and Λ is a weighted pore-volume to surface-area ratio with the weight emphasizing narrowing parts of the connected pore space. It was shown by Johnson et al. (1987) that for a wide range of porous media $M \approx 1$. For the sake of definiteness, $M = 1$ in what follows. The density factors and the damping factor $b_0 B$ always appear together. It is therefore convenient to define complex valued, frequency-dependent density factors $\hat{\rho}_{12} = \rho_{12} + ib_0 B/\omega$, $\hat{\rho}_{11} = \rho_{11} - ib_0 B/\omega$ and $\hat{\rho}_{22} = \rho_{22} - ib_0 B/\omega$.

Considering a stack of poroelastic layers as depicted in Figure 1. At each boundary separating the layers in the stack, six boundary conditions should be satisfied (we have three upgoing and three downgoing waves, as we will see). Assuming welded grain contacts and interconnected pores, the field components in the first-order array

$$\hat{\mathbf{f}}(z) = (\hat{v}_z, \hat{\zeta}_z, \hat{\sigma}_{zx}, \hat{\sigma}_{zz}, \hat{p}, \hat{v}_x)^T, \tag{10}$$

must be continuous, where $\hat{v}_z = i\omega\hat{u}_z$, $\hat{v}_x = i\omega\hat{u}_x$, and $\hat{\zeta}_z = (1-\phi)\hat{v}_z + \phi\hat{w}_z$ for $\hat{w}_z = i\omega\hat{U}_z$. Here, $\hat{}$ denotes transformation of the variables to the (k_x, z, ω)-domain. It is shown in

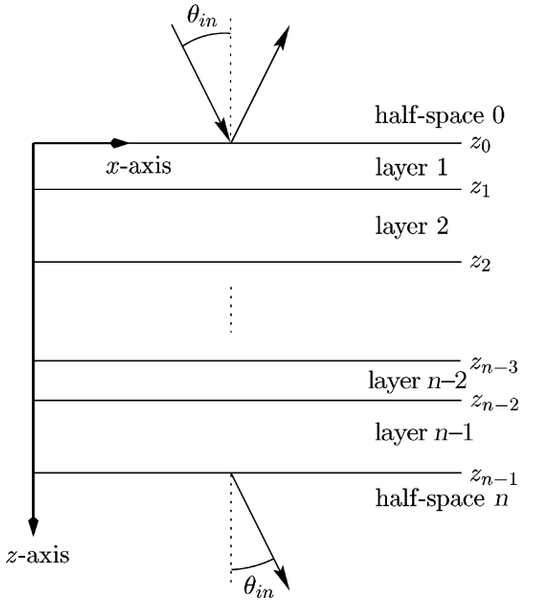

Figure 1. Coordinate system of the multilayered structure. The wave is incident at $z = z_0$.

Appendix A that the equations of motion (6) and (7) can be expanded to yield

$$\frac{\partial \hat{\mathbf{f}}}{\partial z} = i\omega \begin{pmatrix} \mathbf{0} & \mathbf{A_1} \\ \mathbf{A_2} & \mathbf{0} \end{pmatrix} \hat{\mathbf{f}}, \tag{11}$$

where the matrices $\mathbf{A_1}$ and $\mathbf{A_2}$ are symmetric. Drijkoningen et al. (2000) derived similar matrices for incompressible grains ($d\rho_s = 0$). The dispersion relation for the compressional waves $\det(\mathbf{A_1}) = 0$ can effectively be written in terms of $\xi = (k_x/\omega)^2$ as

$$(PR - Q^2)\xi^2 - (P\hat{\rho}_{22} + R\hat{\rho}_{11} - 2Q\hat{\rho}_{12})\xi + (\hat{\rho}_{11}\hat{\rho}_{22} - \hat{\rho}_{12}^2) = 0, \tag{12}$$

where we have defined $P = A + 2\mu$. There are consequently two longitudinal wave modes: the fast and the slow compressional waves, to be indicated p_1 and p_2, respectively. The dispersion relation for the shear wave $\det(\mathbf{A_2}) = 0$ is given by

$$\mu\hat{\rho}_{22}\xi_{sh} - (\hat{\rho}_{11}\hat{\rho}_{22} - \hat{\rho}_{12}^2) = 0. \tag{13}$$

Each wave propagates simultaneously in the pore fluid and in the frame. The fluid to solid amplitude ratios β_{p_1}, β_{p_2}, and β_{sh} are given by

$$\beta_\ell = \frac{\hat{\rho}_{11} - P\xi_\ell}{Q\xi_\ell - \hat{\rho}_{12}}, \quad \text{where } \ell = p_1, p_2, \quad \text{and} \tag{14}$$

$$\beta_{sh} = -\frac{\hat{\rho}_{12}}{\hat{\rho}_{22}}. \tag{15}$$

MATRIX PROPAGATOR METHOD

Let us consider a stack of $(n-1)$ homogeneous poroelastic layers, numbered $1, 2, \cdots (n-1)$, bounded from above and below by two fluid half-spaces which we denote 0 and n, respectively. Assuming an obliquely incident plane acoustic wave, it is required to determine the reflection and transmission from the layer stack (see Figure 1).

Omitting the superscripts $\hat{}$ in the notations, the response $\mathbf{f}$ at a given point in a given layer is the sum of all the various upgoing and downgoing plane waves that are present at that particular location. Following Kennett and Kerry (1979), the first-order array $\boldsymbol{\varphi}$ is defined to contain the various plane wave amplitudes:

$$\boldsymbol{\varphi} = \left(\varphi_{p_1}^+, \varphi_{p_2}^+, \varphi_{sh}^+, -\varphi_{p_1}^-, -\varphi_{p_2}^-, \varphi_{sh}^-\right)^T, \tag{16}$$

and can be written in the partitioned form $\boldsymbol{\varphi} = (\phi^+, \phi^-)^T$, where the $+$ refers to downgoing, and the $-$ to upgoing waves. Similarly, the composition matrix $\mathbf{L}$ is defined to have columns that contain the response of each of the six types of plane waves in a uniform material. Thus, the total material response $\mathbf{f}(z)$ for $z_{j-1} < z < z_j$ is simply

$$\begin{aligned}\mathbf{f}(z) &= \mathbf{L}\,\mathrm{diag}[e^{-i\omega q_{p_1}(z-z_{j-1})}, e^{-i\omega q_{p_2}(z-z_{j-1})}, e^{-i\omega q_{sh}(z-z_{j-1})}, \\ &\qquad e^{i\omega q_{p_1}(z-z_{j-1})}, e^{i\omega q_{p_2}(z-z_{j-1})}, e^{i\omega q_{sh}(z-z_{j-1})}]\boldsymbol{\varphi} \\ &= \mathbf{B}(z, z_{j-1})\boldsymbol{\varphi},\end{aligned} \tag{17}$$

where we denote the coordinate of the upper boundary of layer j by z_{j-1}. The columns of $\mathbf{L}$ are the eigenvectors of the governing equations (11), while the eigenvalues are the vertical wave slownesses q_{p_1}, q_{p_2}, and q_{sh}. The vertical slownesses are related to the complex phase slownesses s_ℓ and the real-valued horizontal slowness s_x as

$$q_\ell^2 + s_x^2 = s_\ell^2, \quad \ell = p_1, p_2, sh. \tag{18}$$

The array $\mathbf{L}$ is given by

$$\mathbf{L} = \omega^2 \begin{pmatrix} \mathbf{L_1} & \mathbf{L_1} \\ \mathbf{L_2} & -\mathbf{L_2} \end{pmatrix}, \tag{19}$$

with

$$\mathbf{L_1} = \begin{pmatrix} q_{p_1} & q_{p_2} & s_x \\ \phi_{p_1} q_{p_1} & \phi_{p_2} q_{p_2} & \phi_{sh} s_x \\ Z_x q_{p_1} & Z_x q_{p_2} & Z_x \gamma_{sh} s_x \end{pmatrix},$$

$$\mathbf{L_2} = \begin{pmatrix} -Z_x\gamma_{p_1}s_x & -Z_x\gamma_{p_2}s_x & Z_x q_{sh} \\ F_{p_1}H_{p_1}s_x & F_{p_2}H_{p_2}s_x & 0 \\ s_x & s_x & -q_{sh} \end{pmatrix}. \tag{20}$$

Here, we have introduced the impedance $Z_x = 2\mu s_x$, slownesses $H_\ell = s_\ell^2/s_x$, and the porosity terms $\phi_\ell = 1 - \phi + \phi\beta_\ell$. Moreover, $\gamma_\ell = 1 - (\lambda_\ell + 2\mu)s_\ell^2/(2\mu s_x^2)$, $\ell = p_1, p_2$. The Lamé coefficients λ_ℓ, $\ell = p_1, p_2$, are related to the Biot coefficients A' and Q' as $\lambda_\ell = A' + Q'\beta_\ell$ (see Appendix A). For the shear wave, we find that $\gamma_{sh} = 1 - s_{sh}^2/(2s_x^2)$. Finally, the fluid compressibility factors $F_\ell = (Q + R\beta_\ell)/\phi$ are defined. Expressions (20) can directly be compared with the expressions by Wang and Kümpel [2003, equations (A-1)–(A-8)] for diffusive poroelastic layers.

From equation (17), it may be seen that for the upper and lower boundaries of the jth layer we can write that

$$\mathbf{f}(z_j) = \mathbf{B}(z_j, z_{j-1})\boldsymbol{\varphi}, \tag{21}$$

$$\mathbf{f}(z_{j-1}) = \mathbf{L}\boldsymbol{\varphi}. \tag{22}$$

From equation (22), it is easily seen that $\mathbf{L}^{-1}\mathbf{f}(z_{j-1}) = \boldsymbol{\varphi}$, which means that from equation (21) it follows that

$$\mathbf{f}(z_j) = \mathbf{B}(z_j, z_{j-1})\mathbf{L}^{-1}\mathbf{f}(z_{j-1}) = \mathbf{H}_j\mathbf{f}(z_{j-1}), \tag{23}$$

where $\mathbf{H}_j$ is the single layer Haskell matrix propagator. Using equation (23) successively, the values of the field vector on the boundaries z_0 and z_{n-1} can be connected:

$$\mathbf{f}(z_{n-1}) = \mathbf{H}(z_{n-1}, z_0)\mathbf{f}(z_0), \tag{24}$$

where $\mathbf{H}(z_{n-1}, z_0) = \mathbf{H}_{n-1} \cdot \mathbf{H}_{n-2} \cdots \mathbf{H}_2 \cdot \mathbf{H}_1$ is called the total matrix propagator and describes wave propagation from the upper interface $z = z_0$ to the lower interface $z = z_{n-1}$.

We now give closed-form analytical expressions of all elements in $\mathbf{H}_j$. From equation (23), it can be seen that the inverse matrix $\mathbf{L}^{-1}$ has to be computed. It reads

$$\mathbf{L}^{-1} = \frac{1}{2}\omega^{-2} \begin{pmatrix} \mathbf{L_1}^{-1} & \mathbf{L_2}^{-1} \\ \mathbf{L_1}^{-1} & -\mathbf{L_2}^{-1} \end{pmatrix}, \tag{25}$$

so that the task of determining the inverse of a 6×6 matrix has been reduced to determining the inverse of two 3×3 matrices

$\mathbf{L}_1$ and $\mathbf{L}_2$. It can be shown that

$$\mathbf{L_1}^{-1} = \begin{pmatrix} \frac{G}{q_{p_1}}\frac{\phi_{p_2}\gamma_{sh}-\phi_{sh}}{\phi_{12}} & \frac{1}{q_{p_1}\phi_{12}} & \frac{1}{s_x}\frac{G}{E_{p_1}}\frac{1}{Z_x}\frac{\phi_{32}}{\phi_{12}} \\ -\frac{G}{q_{p_2}}\frac{\phi_{p_1}\gamma_{sh}-\phi_{sh}}{\phi_{12}} & -\frac{1}{q_{p_2}\phi_{12}} & \frac{1}{s_x}\frac{G}{E_{p_2}}\frac{1}{Z_x}\frac{\phi_{13}}{\phi_{12}} \\ \frac{G}{s_x} & 0 & -\frac{G}{s_x}\frac{1}{Z_x} \end{pmatrix}, \quad (26)$$

$$\mathbf{L_2}^{-1} = \begin{pmatrix} \frac{Z_{p_1}^{-1}}{s_x} & -\frac{Y_{p_1}^{-1}}{s_x} & \frac{Z_x Z_{p_1}^{-1}}{s_x} \\ -\frac{Z_{p_2}^{-1}}{s_x} & \frac{Y_{p_2}^{-1}}{s_x} & -\frac{Z_x Z_{p_2}^{-1}}{s_x} \\ \frac{Z_{p_1}^{-1}-Z_{p_2}^{-1}}{q_{sh}} & -\frac{Y_{p_1}^{-1}-Y_{p_2}^{-1}}{q_{sh}} & \frac{Z_x(Z_{p_1}^{-1}-Z_{p_2}^{-1})-1}{q_{sh}} \end{pmatrix}. \quad (27)$$

Here, we adopt the notation $E_\ell = q_\ell / s_x$ and $G = 2s_x^2/s_{sh}^2$. The porosity difference terms $\phi_{12} = \phi_{p_1} - \phi_{p_2}$, $\phi_{13} = \phi_{p_1} - \phi_{sh}$, and $\phi_{32} = \phi_{sh} - \phi_{p_2}$ are used for brevity. The inverse impedances $Z_{p_1}^{-1} = F_{p_2}/(F\,H_{p_1})$, $Z_{p_2}^{-1} = F_{p_1}/(F\,H_{p_2})$, $Y_{p_1}^{-1} = (\lambda_{p_2}+2\mu)/(F\,H_{p_1})$, and $Y_{p_2}^{-1} = (\lambda_{p_1}+2\mu)/(F\,H_{p_2})$ are defined, where $F = F_{p_2}(\lambda_{p_1}+2\mu) - F_{p_1}(\lambda_{p_2}+2\mu)$. Expressions (26) and (27) can directly be compared with the ones by Wang and Kümpel [2003, equations (A-9)–(A-14)] for diffusive poroelastic media.

From equation (23), the elements of $\mathbf{H}_j$ can now be determined. The analytical expressions are summarized in Appendix B. This is an important result because it allows closed-form analytical expressions for reflection and transmission coefficients to be derived (as we will see).

Global matrix $\mathbf{H}(z_{n-1}, z_0)$ has remarkable properties. From equation (23), it can be seen that $\det(\mathbf{H}_j) = 1$. As the global matrix propagator $\mathbf{H}(z_{n-1}, z_0)$ results from multiplication of the individual matrices $\mathbf{H}_j$, we also find that $\det(\mathbf{H}(z_{n-1}, z_0)) = 1$. Moreover, from equation (24), it can be seen that wave propagation in the opposite direction (from the lower interface to the upper interface) is defined by

$$\mathbf{f}(z_0) = \mathbf{H}(z_0, z_{n-1})\mathbf{f}(z_{n-1}). \quad (28)$$

Combining equations (24) and (28) now yields

$$\mathbf{H}(z_0, z_{n-1}) = \mathbf{H}^{-1}(z_{n-1}, z_0). \quad (29)$$

REFLECTION AND TRANSMISSION

We proceed with the problem of the determination of the reflection and transmission coefficients. The origin of the coordinates is set at the boundary between media 0 and 1, so at $z = z_0$. The z-axis is pointing downwards (Figure 1). Introducing the reflection coefficient $\mathcal{R}$, the total field of the incident and reflected waves in the upper fluid half-space can be characterized by

$$p = \omega^2 \rho_f \left[e^{-i\omega q_f z} + \mathcal{R} e^{i\omega q_f z} \right], \quad (30)$$

$$w_z = \frac{\omega^2 \rho_f}{Z_f} \left[e^{-i\omega q_f z} - \mathcal{R} e^{i\omega q_f z} \right], \quad (31)$$

where Z_f is the acoustic impedance $\rho_f c_f / \cos\theta_{\text{in}}$ of the upper fluid layer and q_f is the vertical fluid slowness. The angle of incidence is denoted θ_{in}. In the lower fluid layer, there will only be waves departing from the boundary, so that the field can be written as

$$p = \omega^2 \rho_f \mathcal{T} e^{-i\omega q_f (z - z_{n-1})}, \quad (32)$$

$$w_z = \frac{\omega^2 \rho_f}{Z_f} \mathcal{T} e^{-i\omega q_f (z - z_{n-1})}, \quad (33)$$

where we have defined the transmission coefficient $\mathcal{T}$. The values of the displacement-stress vector on the exterior boundaries z_{n-1} and z_0 are connected through

$$\left(v_z^{(n-1)}, \zeta_z^{(n-1)}, 0, 0, p^{(n-1)}, v_x^{(n-1)} \right)^T = \mathbf{H}(z_{n-1}, z_0) \cdot \left(v_z^{(0)}, \zeta_z^{(0)}, 0, 0, p^{(0)}, v_x^{(0)} \right)^T. \quad (34)$$

From the third and fourth equations in set (34), the velocities at $z = 0$ (i.e., $v_z^{(0)}$ and $v_x^{(0)}$) can be written in terms of $\zeta_z^{(0)}$ and $p^{(0)}$. Substitution into the second and fifth equations of set (34) then yields

$$\zeta_z^{(n-1)} = M_{22}\zeta_z^{(0)} + M_{25} p^{(0)}, \quad (35)$$

$$p^{(n-1)} = M_{52}\zeta_z^{(0)} + M_{55} p^{(0)}, \quad (36)$$

where

$$\begin{aligned} M_{22} &= H_{22} + H_{21}H_{3462} + H_{26}H_{4312}, \\ M_{25} &= H_{25} + H_{21}H_{3465} + H_{26}H_{4315}, \\ M_{52} &= H_{52} + H_{51}H_{3462} + H_{56}H_{4312}, \\ M_{55} &= H_{55} + H_{51}H_{3465} + H_{56}H_{4315}. \end{aligned} \quad (37)$$

Here, we have adopted the notation $H_{k\ell mn} = (H_{km}H_{\ell n} - H_{\ell m}H_{kn})/(H_{46}H_{31} - H_{36}H_{41})$ where it is stressed that the denominator of $H_{k\ell mn}$ is always identical. Upon term-wise inspection, we find that M_{22} and M_{55} are dimensionless numbers, M_{25} is an inverse impedance, and M_{52} is an impedance.

At the interfaces z_0 and z_{n-1}, continuity of pressure is satisfied. Also continuity of fluid volume flux applies: $\zeta_z = w_z$. Substitution of equations (30)–(33) into equations (35) and (36) now yields

$$\mathcal{R} = \frac{(Z_f M_{22} - M_{52}) + Z_f(Z_f M_{25} - M_{55})}{(Z_f M_{22} - M_{52}) - Z_f(Z_f M_{25} - M_{55})}, \quad (38)$$

$$\mathcal{T} = \frac{2Z_f(M_{22}M_{55} - M_{25}M_{52})}{(Z_f M_{22} - M_{52}) - Z_f(Z_f M_{25} - M_{55})}. \quad (39)$$

Expressions (38) and (39) provide the possibility to analytically compute the reflection and transmission coefficients of a stack of poroelastic layers between two fluid half-spaces without having to resort to numerical matrix inversion and multiplication schemes. For poroelastic media, these expressions are novel and easy to use. However, it is well known that the results based on a direct implementation of expressions (38) and (39) exhibit instabilities due to the loss-of-precision problem which occurs when differently evanescent solutions are numerically coupled. A number of publications attempted to solve this difficulty numerically (Kennett, 1983; Lévesque and Piché, 1992). In what follows, we assess the range of validity of our analytical expressions (38) and (39) through comparison with the numerical reflectivity scheme of Kennett and Kerry (1979).

VALIDITY ASSESSMENT

We consider the case of a normally incident fluid wave upon a stratified medium consisting of three different porous layers bounded from above and below by two fluid half-spaces (see Figure 1). The layer properties are given in Table 1. The fluid in the pores and in the half-spaces is water ($\rho_f = 1000$ kg/m^3, $K_f = 2.2$ GPa, $\eta = 0.001$ Pa·s). The grain bulk modulus is $K_s = 36.6$ GPa for all layers.

For normal incidence, inspection of the terms in Appendix B shows that only 20 out of 36 remain. All others become zero. Introducing the variables $\delta_\ell = \omega q_\ell (z_j - z_{j-1})$, the remaining terms are

$$
\begin{aligned}
h_{11} &= (-\phi_{p_2}\cos\delta_{p_1} + \phi_{p_1}\cos\delta_{p_2})/\phi_{12},\\
h_{12} &= (\cos\delta_{p_1} - \cos\delta_{p_2})/\phi_{12},\\
h_{14} &= -i(F_{p_2}s_{p_2}\sin\delta_{p_1} - F_{p_1}s_{p_1}\sin\delta_{p_2})/(Fs_{p_1}s_{p_2}),\\
h_{15} &= i(s_{p_2}(\lambda_{p_2}+2\mu)\sin\delta_{p_1}\\
&\quad - s_{p_1}(\lambda_{p_1}+2\mu)\sin\delta_{p_2})/(Fs_{p_1}s_{p_2}),\\
h_{21} &= -\phi_{p_1}\phi_{p_2}(\cos\delta_{p_1} - \cos\delta_{p_2})/\phi_{12},\\
h_{22} &= (\phi_{p_1}\cos\delta_{p_1} - \phi_{p_2}\cos\delta_{p_2})/\phi_{12},\\
h_{24} &= -i(F_{p_2}s_{p_2}\phi_{p_1}\sin\delta_{p_1} - F_{p_1}s_{p_1}\phi_{p_2}\sin\delta_{p_2})/(Fs_{p_1}s_{p_2}),\\
h_{25} &= i(s_{p_2}(\lambda_{p_2}+2\mu)\phi_{p_1}\sin\delta_{p_1}\\
&\quad - s_{p_1}(\lambda_{p_1}+2\mu)\phi_{p_2}\sin\delta_{p_2})/(Fs_{p_1}s_{p_2}),\\
h_{33} &= h_{66} = \cos\delta_{sh},\\
h_{36} &= -i\mu s_{sh}\sin\delta_{sh},\\
h_{41} &= i(s_{p_1}(\lambda_{p_1}+2\mu)\phi_{p_2}\sin\delta_{p_1}\\
&\quad - s_{p_2}(\lambda_{p_2}+2\mu)\phi_{p_1}\sin\delta_{p_2})/\phi_{12},\\
h_{42} &= -i(s_{p_1}(\lambda_{p_1}+2\mu)\sin\delta_{p_1}\\
&\quad - s_{p_2}(\lambda_{p_2}+2\mu)\sin\delta_{p_2})/\phi_{12},\\
h_{44} &= (\lambda_{p_1}+2\mu)c_{p_1}H_{p_1}\cos\delta_{p_1}\\
&\quad - (\lambda_{p_2}+2\mu)c_{p_2}H_{p_2}\cos\delta_{p_2},\\
h_{45} &= -(\lambda_{p_1}+2\mu)(\lambda_{p_2}+2\mu)(\cos\delta_{p_1} - \cos\delta_{p_2})/F,\\
h_{51} &= i(F_{p_1}s_{p_1}\phi_{p_2}\sin\delta_{p_1} - F_{p_2}s_{p_2}\phi_{p_1}\sin\delta_{p_2})/\phi_{12},\\
h_{52} &= -i(F_{p_1}s_{p_1}\sin\delta_{p_1} - F_{p_2}s_{p_2}\sin\delta_{p_2})/\phi_{12},\\
h_{54} &= F_{p_1}F_{p_2}(\cos\delta_{p_1} - \cos\delta_{p_2})/F,\\
h_{55} &= -(F_{p_1}(\lambda_{p_2}+2\mu)\cos\delta_{p_1}\\
&\quad - F_{p_2}(\lambda_{p_1}+2\mu)\cos\delta_{p_2})/F,\\
h_{63} &= -i\sin\delta_{sh}/(\mu s_{sh}).
\end{aligned}
\tag{40}
$$

Table 1. Parameters of the three individual porous layers composing the 1-m thick stack. The transmission and reflection coefficients of the stack are shown in Figures 2 and 3.

Layer number	Thickness (m)	ρ_s (kg/m^3)	ϕ %	μ (GPa)	K_b (GPa)	k_0 (darcys)	α_∞
1	0.25	2220	24.0	9.7	15.4	1	2.1
2	0.35	2216	32.0	6.2	7.8	4	1.9
3	0.40	2221	35.5	5.5	6.6	2	2

As the total-stack matrix propagator $\mathbf{H}(z_{n-1}, z_0)$ stems from successive multiplication of the individual layer matrices $\mathbf{H}_j$, we find that $\mathbf{H}(z_{n-1}, z_0)$ will also have 20 nonzero elements at exactly the same position as the layer matrix $\mathbf{H}_j$. From equations (37), we thus find that

$$
\begin{aligned}
M_{22} &= H_{22} - H_{21}H_{42}/H_{41},\\
M_{25} &= H_{25} - H_{21}H_{45}/H_{41},\\
M_{52} &= H_{52} - H_{51}H_{42}/H_{41},\\
M_{55} &= H_{55} - H_{51}H_{45}/H_{41}.
\end{aligned}
\tag{41}
$$

As expected, the shear wave no longer contributes to equations (41). Obviously, definitions (38) and (39) for $\mathcal{R}$ and $\mathcal{T}$ remain the same. We now compare expressions (38) and (39) with Kennett's reflectivity scheme, which is based on an intuitive recursion scheme and is inherently stable because the phase-advancement diagonal matrix only contains elements with amplitudes less than one (Pride et al., 2002) (see Appendix C). The results are plotted in Figures 2 and 3.

We notice that for lower frequencies the analytical results are fully in agreement with the numerical ones. In the limiting case for low frequencies, the transmission coefficient is one, and there is no phase lag. The reflection coefficient goes to zero, and there is a 90° phase lag. The transmission and reflection curves display a characteristic recursive pattern of maxima and minima, which is mainly determined by the λ/d ratio of the p_1 wave. It is also noticed that the maximum transmission values for each cycle tend to decrease as frequency goes up. This is due to the increasing dissipation in the porous layers. Because reflection is not so much associated with propagation through the dissipative stack, the maxima of the reflection coefficient do not show this trend. Notice also that there is no cycle skipping in the phase behavior of the reflection coefficient, whereas this is prominent in the phase plot of the transmittivity.

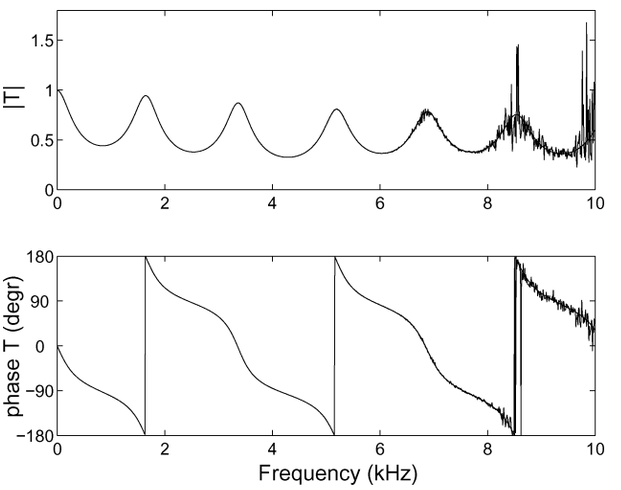

Figure 2. Absolute and phase values of the transmission coefficient of a layered medium, bounded from above and below by fluid half-spaces. The results from the propagator method and the reflectivity method are plotted on top of each other. At high frequencies, the propagator method becomes unstable. The parameters are given in Table 1.

At higher frequencies, the analytical results deviate from the stable numerical predictions due to the loss-of-precision problem described in the previous section, and an unstable behavior is observed for the analytical results. Because the vertical wavenumber has an imaginary part, there are exponentials in the expressions (40) that have large positive arguments. Although in our analytical results, these large exponentials are multiplied by small ones to yield the $\cos\delta_\ell$ and $\sin\delta_\ell$ expressions, the problem is that when one implements the approach on a computer, the large exponentials produce numerical difficulties. For the Biot slow wave, this problem is particularly important because of the relatively large imaginary part of the vertical wavenumber. To illustrate this, we investigate for what single layer thickness h and frequency f the transmittivity becomes unstable (i.e., the relative difference between the analytical expression and Kennett's reflectivity scheme exceeds ε). The results are plotted in Figure 4 (solid lines) for different permeability values. The other layer properties are those of layer 3 (Table 1). We found that the choice for ε hardly influences the results. In Figure 4, $\varepsilon = 0.01$ is used. Also plotted in Figure 4 are the slow-wave curves $-\mathcal{C}/\omega\mathrm{Im}(s_{p_2})$ (dashed lines), where the constants $\mathcal{C}$ are determined by least-squares fits to the corresponding stability curves. It can be seen that the critical layer thickness h equals the slow-wave inverse wavenumber $-\mathcal{C}/\omega\mathrm{Im}(s_{p_2})$ over a wide frequency range, where $\mathcal{C}$ can be identified as the critical exponential value that causes the numerical instabilities. This proves that indeed the slow compressional wave determines the stability of the Haskell method. The critical exponential values $\mathcal{C}$ are given in Table 2. They are computer-precision determined and not so much affected by the layer properties. We also notice that in a typical seismic frequency range (10–100 Hz), the critical (total) layer thickness is on the order of a few meters for permeability values of some 200 mD. This implies that below these critical values there is no need for special numerical treatment, and a direct implementation of the propagator matrix method as in expressions (38) and (39) is sufficient. Above these critical values, methods like the ones suggested by Wang and Kümpel (2003) for slow deformation processes could be used to extend the stability range of the matrix propagator method.

CONCLUSIONS

We fully expanded the Thomson-Haskell propagator matrix method to obtain closed-form analytical expressions for the reflection and transmission coefficients of a horizontally stratified poroelastic medium that is bounded from above and below by fluid half-spaces. The Biot equations governing wave propagation in vertically inhomogeneous porous solids were written as an eigenvalue problem with symmetric off-diagonal submatrices.

The stability of a direct implementation of the propagator matrix method was investigated by comparison with Kennett's reflectivity scheme. We found that below a critical value of a few meters for the total layer thickness, the propagator matrix method is stable in the seismic frequency range (10–100 Hz) for permeability values of some 200 mD.

Moreover, the stability is mainly determined by the imaginary part of the vertical wavenumber of the Biot slow wave because of its relatively large numerical value, and in this way an initial estimate of the numerical stability of the matrix propagator method can easily be made.

Table 2. Critical exponential values $\mathcal{C}$, obtained by the least-squares method.

k_0 (darcys)	$\mathcal{C}$
20	26.2
2	24.9
0.2	23.9
0.02	22.8

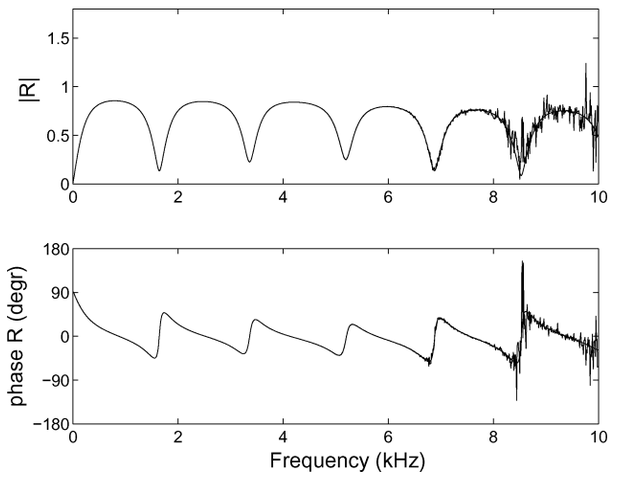

Figure 3. Absolute and phase values of the reflection coefficient of a layered medium, bounded from above and below by fluid half-spaces. The results from the propagator method and the reflectivity method are plotted on top of each other. At high frequencies, the propagator method becomes unstable. The parameters are given in Table 1.

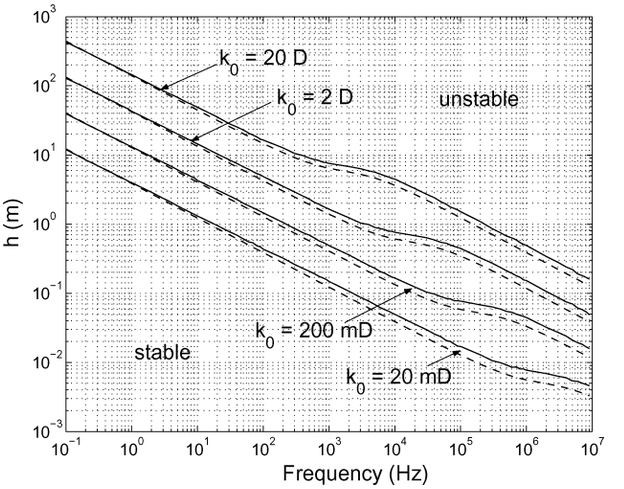

Figure 4. Numerically stable and unstable regions of the single-layer propagator matrix method for different permeability values (solid lines). The other parameter values are given in Table 1, layer 3. Predictions taking only the slow wave into account are indicated by dashed lines.

APPENDIX A

COMPONENTS OF MATRICES $\mathbf{A_1}$ AND $\mathbf{A_2}$

The stress-strain relations for porous media can be written in the following general form (Biot, 1956):

$$-\frac{\partial \sigma_{ij}}{\partial t} = \mu\left(\frac{\partial v_i}{\partial x_j} + \frac{\partial v_j}{\partial x_i}\right) + \left(A'\nabla\cdot\mathbf{v} + Q'\nabla\cdot\mathbf{w}\right)\delta_{ij}, \tag{A-1}$$

$$-\phi\frac{\partial p}{\partial t} = Q\nabla\cdot\mathbf{v} + R\nabla\cdot\mathbf{w}, \tag{A-2}$$

where we have defined $Q' = Q - (1-\phi)R/\phi$ and $A' = A - (1-\phi)Q/\phi$. A, Q, and R are elastic coefficients defined by Biot and Willis (1957), whereas μ denotes the frame shear modulus. For incompressible grains, $Q' = 0$, and A' equals the Lamé parameter λ. The intergranular stresses are denoted σ_{ij}, and they are defined negative in tension. Applying the transformation $\partial/\partial t \to i\omega$ and $\partial/\partial x \to -ik_x$, we find that

$$-i\omega\hat{\sigma}_{zx} = \mu\left(-ik_x\hat{v}_z + \frac{\partial \hat{v}_x}{\partial z}\right), \tag{A-3}$$

$$-i\omega\hat{\sigma}_{xx} = 2\mu(-ik_x\hat{v}_x) + A'\left(-ik_x\hat{v}_x + \frac{\partial \hat{v}_z}{\partial z}\right) + Q'\left(-ik_x\hat{w}_x + \frac{\partial \hat{w}_z}{\partial z}\right), \tag{A-4}$$

$$-i\omega\hat{\sigma}_{zz} = 2\mu\frac{\partial \hat{v}_z}{\partial z} + A'\left(-ik_x\hat{v}_x + \frac{\partial \hat{v}_z}{\partial z}\right) + Q'\left(-ik_x\hat{w}_x + \frac{\partial \hat{w}_z}{\partial z}\right), \tag{A-5}$$

$$-i\omega\phi\hat{p} = Q\left(-ik_x\hat{v}_x + \frac{\partial \hat{v}_z}{\partial z}\right) + R\left(-ik_x\hat{w}_x + \frac{\partial \hat{w}_z}{\partial z}\right). \tag{A-6}$$

The momentum equations for the solid and the fluid can be written in the x- and z-directions as

$$i\omega(\hat{\rho}_{11}\hat{v}_x + \hat{\rho}_{12}\hat{w}_x) = ik_x\hat{\sigma}_{xx} - \frac{\partial \hat{\sigma}_{zx}}{\partial z} + ik_x(1-\phi)\hat{p}, \tag{A-7}$$

$$i\omega(\hat{\rho}_{11}\hat{v}_z + \hat{\rho}_{12}\hat{w}_z) = -\frac{\partial \hat{\sigma}_{zz}}{\partial z} + ik_x\hat{\sigma}_{xz} - (1-\phi)\frac{\partial \hat{p}}{\partial z}, \tag{A-8}$$

$$i\omega(\hat{\rho}_{12}\hat{v}_x + \hat{\rho}_{22}\hat{w}_x) = ik_x\phi\hat{p}, \tag{A-9}$$

$$i\omega(\hat{\rho}_{12}\hat{v}_z + \hat{\rho}_{22}\hat{w}_z) = -\phi\frac{\partial \hat{p}}{\partial z}. \tag{A-10}$$

Here we have used the notation that $\hat{\rho}_{nn} = \rho_{nn} - ib(\omega)/\omega$ for $n = 1, 2$ and that $\hat{\rho}_{12} = \rho_{12} + ib(\omega)/\omega$, where $b(\omega) = b_0 B$ is the dynamic interaction coefficient (Johnson et al., 1987).

Our goal is to derive the six expressions of equation (11). Combining equations (A-5) and (A-6), and using equation (A-9) for $\hat{w}_x$, it can be found that

$$\frac{\partial \hat{v}_z}{\partial z} = -i\omega\frac{R}{D}\hat{\sigma}_{zz} + i\omega\phi\hat{p}\frac{Q'}{D} + ik_x\hat{v}_x\left(1 - \frac{2\mu R}{D}\right), \tag{A-11}$$

$$\frac{\partial \hat{w}_z}{\partial z} = i\omega\frac{Q}{D}\hat{\sigma}_{zz} + i\omega\phi\hat{p}\left(\frac{k_x^2}{\omega^2}\frac{1}{\hat{\rho}_{22}} - \frac{P'}{D}\right) + ik_x\hat{v}_x\left(-\frac{\hat{\rho}_{12}}{\hat{\rho}_{22}} + \frac{2\mu Q}{D}\right), \tag{A-12}$$

where we have defined $P' = A' + 2\mu$, and the denominator $D = RP' - QQ'$. For incompressible grains, P' represents the constrained modulus or plain-wave modulus $\lambda + 2\mu$. It is now convenient to define the velocity $\hat{\zeta}_z$, which represents the fluid volume flux with respect to a moving solid boundary:

$$\hat{\zeta}_z = (1-\phi)\hat{v}_z + \phi\hat{w}_z. \tag{A-13}$$

We can write in linearized form that

$$\frac{\partial \hat{\zeta}_z}{\partial z} = (1-\phi)\frac{\partial \hat{v}_z}{\partial z} + \phi\frac{\partial \hat{w}_z}{\partial z} = i\omega\phi\frac{Q'}{D}\hat{\sigma}_{zz} + i\omega\phi\hat{p}\left[\frac{k_x^2}{\omega^2}\frac{\phi}{\hat{\rho}_{22}} - \frac{\phi P'}{D} + \frac{(1-\phi)Q'}{D}\right] + ik_x\hat{v}_x\left[\frac{(1-\phi)\hat{\rho}_{22} - \phi\hat{\rho}_{12}}{\hat{\rho}_{22}} + \frac{2\mu\phi Q'}{D}\right]. \tag{A-14}$$

Substituting equations (A-11) and (A-12) into equation (A-4), and using again equation (A-9) for $\hat{w}_x$, we find that

$$\hat{\sigma}_{xx} = \left(1 - \frac{2\mu R}{D}\right)\hat{\sigma}_{zz} + \phi\hat{p}\frac{2\mu Q'}{D} + 4\mu\hat{v}_x\frac{k_x}{\omega}\left(1 - \frac{\mu R}{D}\right). \tag{A-15}$$

From equation (A-7), it now follows that

$$\frac{\partial \hat{\sigma}_{zx}}{\partial z} = ik_x\hat{\sigma}_{zz}\left(1 - \frac{2\mu R}{D}\right) + ik_x\hat{p}\left[\frac{(1-\phi)\hat{\rho}_{22} - \phi\hat{\rho}_{12}}{\rho_{22}} + \frac{2\mu\phi Q'}{D}\right] = i\omega\hat{v}_x\left[4\mu\frac{k_x^2}{\omega^2}\left(1 - \frac{\mu R}{D}\right) + \frac{\hat{\rho}_{12}^2 - \hat{\rho}_{11}\hat{\rho}_{22}}{\hat{\rho}_{22}}\right]. \tag{A-16}$$

Using equation (A-13) to eliminate $\hat{w}_z$, it follows from equation (A-10) that

$$\frac{\partial \hat{p}}{\partial z} = i\omega\hat{v}_z\left(\frac{1-\phi}{\phi^2}\hat{\rho}_{22} - \frac{\hat{\rho}_{12}}{\phi}\right) - \frac{i\omega}{\phi^2}\hat{\rho}_{22}\hat{\zeta}_z. \tag{A-17}$$

Substituting equation (A-17) into equation (A-8), and again using equation (A-13) to eliminate $\hat{w}_z$, now easily yields

$$\frac{\partial \hat{\sigma}_{zz}}{\partial z} = i\omega\hat{v}_z\left[\frac{2(1-\phi)}{\phi}\hat{\rho}_{12} - \frac{(1-\phi)^2}{\phi^2}\hat{\rho}_{22} - \hat{\rho}_{11}\right] + i\omega\hat{\zeta}_z\left[\frac{(1-\phi)}{\phi^2}\hat{\rho}_{22} - \frac{\hat{\rho}_{12}}{\phi}\right]. + ik_x\hat{\sigma}_{xz}. \tag{A-18}$$

Finally, we observe that the relation for $\partial\hat{v}_x/\partial z$ is provided by equation (A-3).

Matrices $\mathbf{A_1}$ and $\mathbf{A_2}$ as specified in equation (11) can now be composed of equations (A-3), (A-11), (A-14), (A-16), (A-17),

and (A-18). It is concluded that both matrices are symmetric and given by

$$\mathbf{A_1} = \begin{pmatrix} -\frac{R}{D} & \cdots & \cdots \\ \frac{\phi Q'}{D} & \frac{k_x^2}{\omega^2}\frac{\phi^2}{\hat{\rho}_{22}} - \frac{\phi^2 P'}{D} + \frac{\phi(1-\phi)Q'}{D} & \cdots \\ \frac{k_x}{\omega}\left(1 - \frac{2\mu R}{D}\right) & \frac{k_x}{\omega}\left(1 - \phi - \phi\frac{\hat{\rho}_{12}}{\hat{\rho}_{22}} + \frac{2\mu\phi Q'}{D}\right) & 4\mu\frac{k_x^2}{\omega^2}\left(1 - \frac{\mu R}{D}\right) + \frac{\hat{\rho}_{12}^2}{\hat{\rho}_{22}} - \hat{\rho}_{11} \end{pmatrix}, \tag{A-19}$$

$$\mathbf{A_2} = \begin{pmatrix} \frac{2(1-\phi)}{\phi}\hat{\rho}_{12} - \frac{(1-\phi)^2}{\phi^2}\hat{\rho}_{22} - \hat{\rho}_{11} & \cdots & \cdots \\ \frac{(1-\phi)}{\phi^2}\hat{\rho}_{22} - \frac{\hat{\rho}_{12}}{\phi} & -\frac{\hat{\rho}_{22}}{\phi^2} & \cdots \\ \frac{k_x}{\omega} & 0 & -\frac{1}{\mu} \end{pmatrix}. \tag{A-20}$$

APPENDIX B

COMPONENTS OF THE SINGLE-LAYER MATRIX PROPAGATOR

Defining the variables $\delta_\ell = \omega q_\ell (z_j - z_{j-1})$ for $\ell = p_1, p_2, sh$, the elements of the single layer Haskell matrix propagator $\mathbf{H}_j$ are:

$$h_{11} = G\left(\frac{\phi_{p_2}\gamma_{sh} - \phi_{sh}}{\phi_{12}}\cos\delta_{p_1} - \frac{\phi_{p_1}\gamma_{sh} - \phi_{sh}}{\phi_{12}}\cos\delta_{p_2} + \cos\delta_{sh}\right),$$

$$h_{12} = \frac{\cos\delta_{p_1} - \cos\delta_{p_2}}{\phi_{12}},$$

$$h_{13} = \frac{G}{Z_x}\left(\frac{\phi_{32}}{\phi_{12}}\cos\delta_{p_1} + \frac{\phi_{13}}{\phi_{12}}\cos\delta_{p_2} - \cos\delta_{sh}\right),$$

$$h_{14} = -i\left(E_{p_1}Z_{p_1}^{-1}\sin\delta_{p_1} - E_{p_2}Z_{p_2}^{-1}\sin\delta_{p_2} + \frac{Z_{p_1}^{-1} - Z_{p_2}^{-1}}{E_{sh}}\sin\delta_{sh}\right),$$

$$h_{15} = i\left(E_{p_1}Y_{p_1}^{-1}\sin\delta_{p_1} - E_{p_2}Y_{p_2}^{-1}\sin\delta_{p_2} + \frac{Y_{p_1}^{-1} - Y_{p_2}^{-1}}{E_{sh}}\sin\delta_{sh}\right),$$

$$h_{16} = -i\left(E_{p_1}Z_{p_1}^{-1}Z_x\sin\delta_{p_1} - E_{p_2}Z_{p_2}^{-1}Z_x\sin\delta_{p_2} + \frac{Z_x\left(Z_{p_1}^{-1} - Z_{p_2}^{-1}\right) - 1}{E_{sh}}\sin\delta_{sh}\right),$$

$$h_{21} = G\left(\frac{\phi_{p_2}\gamma_{sh} - \phi_{sh}}{\phi_{12}}\phi_{p_1}\cos\delta_{p_1} - \frac{\phi_{p_1}\gamma_{sh} - \phi_{sh}}{\phi_{12}}\phi_{p_2}\cos\delta_{p_2} + \phi_{sh}\cos\delta_{sh}\right),$$

$$h_{22} = \frac{\phi_{p_1}\cos\delta_{p_1} - \phi_{p_2}\cos\delta_{p_2}}{\phi_{12}},$$

$$h_{23} = \frac{G}{Z_x}\left(\frac{\phi_{32}}{\phi_{12}}\phi_{p_1}\cos\delta_{p_1} + \frac{\phi_{13}}{\phi_{12}}\phi_{p_2}\cos\delta_{p_2} - \phi_{sh}\cos\delta_{sh}\right),$$

$$h_{24} = -i\left(E_{p_1}Z_{p_1}^{-1}\phi_{p_1}\sin\delta_{p_1} - E_{p_2}Z_{p_2}^{-1}\phi_{p_2}\sin\delta_{p_2} + \frac{Z_{p_1}^{-1} - Z_{p_2}^{-1}}{E_{sh}}\phi_{sh}\sin\delta_{sh}\right),$$

$$h_{25} = i\left(E_{p_1}Y_{p_1}^{-1}\phi_{p_1}\sin\delta_{p_1} - E_{p_2}Y_{p_2}^{-1}\phi_{p_2}\sin\delta_{p_2} + \frac{Y_{p_1}^{-1} - Y_{p_2}^{-1}}{E_{sh}}\phi_{sh}\sin\delta_{sh}\right),$$

$$h_{26} = -i\left(E_{p_1}Z_{p_1}^{-1}Z_x\phi_{p_1}\sin\delta_{p_1} - E_{p_2}Z_{p_2}^{-1}Z_x\phi_{p_2}\sin\delta_{p_2} + \frac{Z_x\left(Z_{p_1}^{-1} - Z_{p_2}^{-1}\right) - 1}{E_{sh}}\phi_{sh}\sin\delta_{sh}\right),$$

This approach is completely analogous to Ursin (1983) for non-porous elastic media.

$$h_{31} = G Z_x \left(\frac{\phi_{p_2}\gamma_{sh} - \phi_{sh}}{\phi_{12}} \cos\delta_{p_1} - \frac{\phi_{p_1}\gamma_{sh} - \phi_{sh}}{\phi_{12}} \cos\delta_{p_2} + \gamma_{sh} \cos\delta_{sh} \right),$$

$$h_{32} = \frac{Z_x}{\phi_{12}} \left(\cos\delta_{p_1} - \cos\delta_{p_2} \right),$$

$$h_{33} = G \left(\frac{\phi_{32}}{\phi_{12}} \cos\delta_{p_1} + \frac{\phi_{13}}{\phi_{12}} \cos\delta_{p_2} - \gamma_{sh} \cos\delta_{sh} \right),$$

$$h_{34} = -i Z_x \left(E_{p_1} Z_{p_1}^{-1} \sin\delta_{p_1} - E_{p_2} Z_{p_2}^{-1} \sin\delta_{p_2} + \gamma_{sh} \frac{Z_{p_1}^{-1} - Z_{p_2}^{-1}}{E_{sh}} \sin\delta_{sh} \right),$$

$$h_{35} = i Z_x \left(E_{p_1} Y_{p_1}^{-1} \sin\delta_{p_1} - E_{p_2} Y_{p_2}^{-1} \sin\delta_{p_2} + \gamma_{sh} \frac{Y_{p_1}^{-1} - Y_{p_2}^{-1}}{E_{sh}} \sin\delta_{sh} \right),$$

$$h_{36} = -i Z_x \left(E_{p_1} Z_{p_1}^{-1} Z_x \sin\delta_{p_1} - E_{p_2} Z_{p_2}^{-1} Z_x \sin\delta_{p_2} + \gamma_{sh} \frac{Z_x \left(Z_{p_1}^{-1} - Z_{p_2}^{-1} \right) - 1}{E_{sh}} \sin\delta_{sh} \right),$$

$$h_{41} = i G Z_x \left(\frac{\phi_{p_2}\gamma_{sh} - \phi_{sh}}{\phi_{12}} \gamma_{p_1} \frac{\sin\delta_{p_1}}{E_{p_1}} - \frac{\phi_{p_1}\gamma_{sh} - \phi_{sh}}{\phi_{12}} \gamma_{p_2} \frac{\sin\delta_{p_2}}{E_{p_2}} - E_{sh} \sin\delta_{sh} \right),$$

$$h_{42} = i \frac{Z_x}{\phi_{12}} \left(\gamma_{p_1} \frac{\sin\delta_{p_1}}{E_{p_1}} - \gamma_{p_2} \frac{\sin\delta_{p_2}}{E_{p_2}} \right),$$

$$h_{43} = i G \left(\frac{\phi_{32}}{\phi_{12}} \gamma_{p_1} \frac{\sin\delta_{p_1}}{E_{p_1}} + \frac{\phi_{13}}{\phi_{12}} \gamma_{p_2} \frac{\sin\delta_{p_2}}{E_{p_2}} + E_{sh} \sin\delta_{sh} \right),$$

$$h_{44} = -Z_x \left(Z_{p_1}^{-1} \gamma_{p_1} \cos\delta_{p_1} - Z_{p_2}^{-1} \gamma_{p_2} \cos\delta_{p_2} - \left(Z_{p_1}^{-1} - Z_{p_2}^{-1} \right) \cos\delta_{sh} \right),$$

$$h_{45} = Z_x \left(Y_{p_1}^{-1} \gamma_{p_1} \cos\delta_{p_1} - Y_{p_2}^{-1} \gamma_{p_2} \cos\delta_{p_2} - \left(Y_{p_1}^{-1} - Y_{p_2}^{-1} \right) \cos\delta_{sh} \right),$$

$$h_{46} = -Z_x \left(Z_x Z_{p_1}^{-1} \gamma_{p_1} \cos\delta_{p_1} - Z_x Z_{p_2}^{-1} \gamma_{p_2} \cos\delta_{p_2} - \left[Z_x \left(Z_{p_1}^{-1} - Z_{p_2}^{-1} \right) - 1 \right] \cos\delta_{sh} \right),$$

$$h_{51} = -i G \left(\frac{\phi_{p_2}\gamma_{sh} - \phi_{sh}}{\phi_{12}} F_{p_1} H_{p_1} \frac{\sin\delta_{p_1}}{E_{p_1}} - \frac{\phi_{p_1}\gamma_{sh} - \phi_{sh}}{\phi_{12}} F_{p_2} H_{p_2} \frac{\sin\delta_{p_2}}{E_{p_2}} \right),$$

$$h_{52} = -\frac{i}{\phi_{12}} \left(F_{p_1} H_{p_1} \frac{\sin\delta_{p_1}}{E_{p_1}} - F_{p_2} H_{p_2} \frac{\sin\delta_{p_2}}{E_{p_2}} \right),$$

$$h_{53} = -\frac{i G}{Z_x} \left(\frac{\phi_{32}}{\phi_{12}} F_{p_1} H_{p_1} \frac{\sin\delta_{p_1}}{E_{p_1}} + \frac{\phi_{13}}{\phi_{12}} F_{p_2} H_{p_2} \frac{\sin\delta_{p_2}}{E_{p_2}} \right),$$

$$h_{54} = F_{p_1} H_{p_1} Z_{p_1}^{-1} \cos\delta_{p_1} - F_{p_2} H_{p_2} Z_{p_2}^{-1} \cos\delta_{p_2},$$

$$h_{55} = -F_{p_1} H_{p_1} Y_{p_1}^{-1} \cos\delta_{p_1} + F_{p_2} H_{p_2} Y_{p_2}^{-1} \cos\delta_{p_2},$$

$$h_{56} = Z_x \left(F_{p_1} H_{p_1} Z_{p_1}^{-1} \cos\delta_{p_1} - F_{p_2} H_{p_2} Z_{p_2}^{-1} \cos\delta_{p_2} \right),$$

$$h_{61} = -i G \left(\frac{\phi_{p_2}\gamma_{sh} - \phi_{sh}}{\phi_{12}} \frac{\sin\delta_{p_1}}{E_{p_1}} - \frac{\phi_{p_1}\gamma_{sh} - \phi_{sh}}{\phi_{12}} \frac{\sin\delta_{p_2}}{E_{p_2}} - E_{sh} \sin\delta_{sh} \right),$$

$$h_{62} = -\frac{i}{\phi_{12}} \left(\frac{\sin\delta_{p_1}}{E_{p_1}} - \frac{\sin\delta_{p_2}}{E_{p_2}} \right),$$

$$h_{63} = -\frac{i G}{Z_x} \left(\frac{\phi_{32}}{\phi_{12}} \frac{\sin\delta_{p_1}}{E_{p_1}} + \frac{\phi_{13}}{\phi_{12}} \frac{\sin\delta_{p_2}}{E_{p_2}} + E_{sh} \sin\delta_{sh} \right),$$

$$h_{64} = Z_{p_1}^{-1} \cos\delta_{p_1} - Z_{p_2}^{-1} \cos\delta_{p_2} - \left(Z_{p_1}^{-1} - Z_{p_2}^{-1} \right) \cos\delta_{sh},$$

$$h_{65} = -Y_{p_1}^{-1} \cos\delta_{p_1} + Y_{p_2}^{-1} \cos\delta_{p_2} + \left(Y_{p_1}^{-1} - Y_{p_2}^{-1} \right) \cos\delta_{sh},$$

$$h_{66} = Z_x Z_{p_1}^{-1} \cos\delta_{p_1} - Z_x Z_{p_2}^{-1} \cos\delta_{p_2} - \left[Z_x \left(Z_{p_1}^{-1} - Z_{p_2}^{-1} \right) - 1 \right] \cos\delta_{sh}.$$

A check on the computation of these 36 elements is provided by $\det(\mathbf{H}_j)=1$. Denoting between parentheses the possible choices for indices i and j of h_{ij}, the elements $h_{\{1,2,6\}\{1,2,6\}}$ and $h_{\{3,4,5\}\{3,4,5\}}$ are dimensionless numbers. The elements $h_{\{1,2,6\}\{3,4,5\}}$ are inverse impedances, and the elements $h_{\{3,4,5\}\{1,2,6\}}$ are impedances.

The above expressions have been computer-coded into `Matlab` and `Maple` and are freely available through the corresponding addresses of the authors.

APPENDIX C

KENNETT'S REFLECTIVITY SCHEME

Following Pride et al. (2002), the response of a stack with topmost interface z_{j-1} is constructed iteratively by application of the recursive scheme

$$\mathcal{R}_{j-1} = R^+_{j-1} + T^-_{j-1}\bar{\mathcal{R}}_j\left(I - R^-_{j-1}\bar{\mathcal{R}}_j\right)^{-1}T^+_{j-1}, \quad \text{(C-1)}$$

$$\mathcal{T}_{j-1} = \bar{\mathcal{T}}_j\left(I - R^-_{j-1}\bar{\mathcal{R}}_j\right)^{-1}T^+_{j-1}, \quad \text{(C-2)}$$

$$\bar{\mathcal{R}}_j = E_j\mathcal{R}_jE_j, \quad \text{(C-3)}$$

$$\bar{\mathcal{T}}_j = \mathcal{T}_jE_j, \quad \text{(C-4)}$$

where $\mathcal{R}_j$ and $\mathcal{T}_j$ are the total-reflection matrix and the total-transmission matrix of the stack with topmost interface z_j (see Figure 1). The iteration begins with $j=n-1$, $\mathcal{R}_{n-1}=R^+_{n-1}$, and $\mathcal{T}_{n-1}=T^+_{n-1}$, and then counts backwards (adds layers) to $j=0$. It uses the downward and upward reflection and transmission matrices $R^{+,-}_j$ and $T^{+,-}_j$ for each isolated interface z_j as well as the phase-advancement diagonal matrix E_j for each layer j defined as:

$$E_j = \operatorname{diag}[e^{-i\omega q_{p_1}(z_j-z_{j-1})}, e^{-i\omega q_{p_2}(z_j-z_{j-1})}, e^{-i\omega q_{sh}(z_j-z_{j-1})}]. \quad \text{(C-5)}$$

The downward transmission and reflection matrices are obtained by writing the plane-wave amplitude just above an interface z_j in the partitioned form as $(1,\phi^-)^T$ and just below the interface as $(\phi^+,0)^T$, so that the downward reflection and transmission matrices are defined by $\phi^- = R^+_j\cdot 1$ and $\phi^+ = T^+_j\cdot 1$. Now using the condition that $\mathbf{f}$ is constant over the interface and the definition $\mathbf{f}=\mathbf{L}\varphi$, we find that

$$R^+_j = \left[\mathbf{L_2}^{-1}_{,j+1}\mathbf{L_2}_{,j} + \mathbf{L_1}^{-1}_{,j+1}\mathbf{L_1}_{,j}\right]^{-1} \times \left[\mathbf{L_2}^{-1}_{,j+1}\mathbf{L_2}_{,j} - \mathbf{L_1}^{-1}_{,j+1}\mathbf{L_1}_{,j}\right], \quad \text{(C-6)}$$

$$T^+_j = \mathbf{L_1}^{-1}_{,j+1}\mathbf{L_1}_{,j}\left[\mathbf{I} + R^+_j\right], \quad \text{(C-7)}$$

where $\mathbf{I}$ is a 3×3 identity matrix. Because of the symmetry in $\mathbf{L}$, these expressions are somewhat more compact than in Pride et al. (2002).

The upward transmission and reflection matrices are similarly defined by imposing upward waves incident from below at the same interface:

$$R^-_j = \left[\mathbf{L_2}^{-1}_{,j}\mathbf{L_2}_{,j+1} + \mathbf{L_1}^{-1}_{,j}\mathbf{L_1}_{,j+1}\right]^{-1} \times \left[\mathbf{L_2}^{-1}_{,j}\mathbf{L_2}_{,j+1} - \mathbf{L_1}^{-1}_{,j}\mathbf{L_1}_{,j+1}\right], \quad \text{(C-8)}$$

$$T^-_j = \mathbf{L_1}^{-1}_{,j}\mathbf{L_1}_{,j+1}\left[\mathbf{I} + R^-_j\right]. \quad \text{(C-9)}$$

Additional care is needed for the construction of the reflection and transmission matrices of the two fluid-porous solid interfaces, due to the absence of a shear and slow compressional wave in the fluid. As suggested by Kennett and Kerry (1979), the following formalism is used:

$$R^+_{n-1} = \begin{pmatrix} R_{p_1^+,p_1^-} & R_{p_2^+,p_1^-} & R_{sh^+,p_1^-} \\ R_{p_1^+,p_2^-} & R_{p_2^+,p_2^-} & R_{sh^+,p_2^-} \\ R_{p_1^+,sh^-} & R_{p_2^+,sh^-} & R_{sh^+,sh^-} \end{pmatrix},$$

$$T^+_{n-1} = \begin{pmatrix} T_{p_1^+,f^+} & T_{p_2^+,f^+} & T_{sh^+,f^+} \\ 0 & 0 & 0 \\ 0 & 0 & 0 \end{pmatrix}, \quad \text{(C-10)}$$

for the downward reflection and transmission matrices at the lower fluid-solid interface and

$$R^+_0 = \begin{pmatrix} R_{f^+,f^-} & 0 & 0 \\ 0 & 0 & 0 \\ 0 & 0 & 0 \end{pmatrix}$$

$$R^-_0 = \begin{pmatrix} R_{p_1^-,p_1^+} & R_{p_2^-,p_1^+} & R_{sh^-,p_1^+} \\ R_{p_1^-,p_2^+} & R_{p_2^-,p_2^+} & R_{sh^-,p_2^+} \\ R_{p_1^-,sh^+} & R_{p_2^-,sh^+} & R_{sh^-,sh^+} \end{pmatrix},$$

$$T^+_0 = \begin{pmatrix} T_{f^+,p_1^+} & 0 & 0 \\ T_{f^+,p_2^+} & 0 & 0 \\ T_{f^+,s^+} & 0 & 0 \end{pmatrix}$$

$$T^-_0 = \begin{pmatrix} T_{p_1^-,f^-} & T_{p_2^-,f^-} & T_{sh^-,f^-} \\ 0 & 0 & 0 \\ 0 & 0 & 0 \end{pmatrix}, \quad \text{(C-11)}$$

for the upward and downward reflection and transmission matrices at the upper fluid-solid interface.

REFERENCES

Biot, M., 1956, Theory of propagation of elastic waves in a fluid-saturated porous solid: Journal of the Acoustical Society of America, **28**, 168–191.

Biot, M., and Willis, D., 1957, The elastic coefficients of the theory of consolidation: Journal of Applied Mechanics, **24**, 594–601.

Drijkoningen, G., Kempen, M. V., and Denneman, A., 2000, Layer matrices for wave propagation in porous media: Petrophysics meets Geophysics: European Association of Geoscientists and Engineers and Société pour l'Avancement de l'Interprétation des Diagraphies, 1–8.

Gurevich, B., and Kelder, O., and Smeulders, D., 1999, Validation of the slow compressional wave in porous media: Comparison of experiments and numerical simulations: Transport in Porous Media, **36**, 149–160.

Haartsen, M., and Pride, S., 1997, Electroseismic waves from point sources in layered media: Journal of Geophysical Research, **102**, 24 745–24 769.

Haskell, N., 1953, The dispersion of surface waves in multilayered media: Bulletin of the Seismological Society of America, **43**, 17–34.

Johnson, D., Koplik, J., and Dashen, R., 1987, Theory of dynamic permeability and tortuosity in fluid-saturated porous media: Journal of Fluid Mechanics, **176**, 379–402.

Kennett, B., 1983, Seismic wave propagation in stratified media: Cambridge University Press.

Kennett, B., and Kerry, N., 1979, Seismic waves in a stratified half space: Geophysical Journal of the Royal Astronomical Society, **57**, 557–583.

Lévesque, G., and Piché, L., 1992, A robust transfer matrix formulation for the ultrasonic response of multilayered absorbing media: Journal of the Acoustical Society of America, **92**, 452–467.
Pride, S., Tromeur, E., and Berryman, J., 2002, Biot slow-wave effects in stratified rock: Geophysics, **67**, 271–281.
Schmidt, H., and Jensen, F., 1985, A full wave solution for propagation in multilayered viscoelastic media with application to Gaussian beam reflection at fluid-solid interfaces: Journal of the Acoustical Society of America, **77**, 813–825.
Schmidt, H., and Tango, G., 1986, Efficient global matrix approach to the computation of synthetic seismograms: Geophysical Journal of the Royal Astronomical Society, **84**, 331–359.
Shapiro, S., Zien, H., and Hubral, P., 1994, A generalized O'Doherty-Anstey formula for waves in finely layered media: Geophysics, **59**, 1750–1762.
Thomson, W., 1950, Transmission of elastic waves through a stratified solid medium: Journal of Applied Physics, 1950, **21**, 89–93.
Ursin, B., 1983, Review of elastic and electromagnetic wave propagation in horizontally layered media: Geophysics, **48**, 1063–1081.
Wang, R., and Kümpel, H., 2003, Poroelasticity: Efficient modeling of strongly coupled slow deformation processes in a multilayered half-space: Geophysics, **68**, 705–717.